Development/Plasticity/Repair

Partial Restoration of Cardiovascular Function by Embryonic Neural Stem Cell Grafts after Complete Spinal Cord Transection

Shaoping Hou,[1,4] Veronica J. Tom,[4] Lori Graham,[1] Paul Lu,[1,2] and Armin Blesch[1,3]

[1]Department of Neurosciences, University of California, San Diego, La Jolla, California 92093, [2]Veterans Administration Medical Center, San Diego, California 92161, [3]Spinal Cord Injury Center, Heidelberg University Hospital, D-69118 Heidelberg, Germany, [4]Spinal Cord Research Center, Department of Neurobiology and Anatomy, Drexel University College of Medicine, Philadelphia, Pennsylvania 19129

High-level spinal cord injury can lead to cardiovascular dysfunction, including disordered hemodynamics at rest and autonomic dysreflexia during noxious stimulation. To restore supraspinal control of sympathetic preganglionic neurons (SPNs), we grafted embryonic brainstem-derived neural stem cells (BS-NSCs) or spinal cord-derived neural stem cells (SC-NSCs) expressing green fluorescent protein into the T4 complete transection site of adult rats. Animals with injury alone served as controls. Implanting of BS-NSCs but not SC-NSCs resulted in recovery of basal cardiovascular parameters, whereas both cell grafts alleviated autonomic dysreflexia. Subsequent spinal cord retransection above the graft abolished the recovery of basal hemodynamics and reflexic response. BS-NSC graft-derived catecholaminergic and serotonergic neurons showed remarkable long-distance axon growth and topographical innervation of caudal SPNs. Anterograde tracing indicated growth of medullar axons into stem cell grafts and formation of synapses. Thus, grafted embryonic brainstem-derived neurons can act as functional relays to restore supraspinal regulation of denervated SPNs, thereby contributing to cardiovascular functional improvement.

Introduction

Spinal cord injury (SCI) usually interrupts supraspinal projections, resulting not only in the loss of motor and sensory control but also in a dysregulated autonomic nervous system. The latter has received more attention in recent years because autonomic dysfunction is a potentially life-threatening condition that severely impairs the quality of life for individuals with cervical and high thoracic SCI (Karlsson, 2006; Weaver et al., 2006; Krassioukov et al., 2007). In the cardiovascular system, the loss of inhibitory control from higher centers alters tonic activity of sympathetic preganglionic neurons (SPNs) in the spinal cord and causes abnormal basal hemodynamics (Teasell et al., 2000; Furlan et al., 2003). Serious autonomic dysreflexia defined by episodes of hypertension and baroreceptor reflex-mediated bradycardia in response to noxious stimuli below the injury level often develops as a result of an abrupt, massive activation of SPNs (Lindan et al., 1980; Krassioukov et al., 2003).

Previous studies have characterized supraspinal neurons and the vasomotor pathways important for the regulation of sympathetic outflow in the spinal cord. Most of these neurons are located in the brainstem (Jansen et al., 1995) and are highly organized and integrated to cooperatively modulate spinal autonomic neurons. Injury-induced intraspinal plasticity and pelvic afferent sprouting have been correlated to the development of chronic autonomic dysreflexia (Cameron et al., 2006; Hou et al., 2008). However, the disruption of descending vasomotor projections after SCI is the fundamental underlying cause of sympathetic neuronal dysfunction and cardiovascular abnormalities. Therefore, regaining supraspinal control to SPNs might be able to restore sympathetic activity and improve hemodynamic performance.

The transplantation of neural stem cells (NSCs) and neuronal progenitors may rebuild injured spinal circuits and repair functional deficits. Although the implantation of embryonic neural tissue or NSCs has been well established over decades, the method still requires additional improvement for achieving satisfactory survival, a high-degree of integration, and long-distance axonal elongation (Reier et al., 1986; Jakeman and Reier, 1991). Taking advantage of a transgenic animal line with green fluorescent protein (GFP) ubiquitously expressed, technical limitations of distinguishing donor cells and their extensions from host tissue can now be overcome (Kisseberth et al., 1999; Gaillard et al., 2007). Recently, we grafted embryonic spinal cord-derived NSCs (SC-NSCs) to the adult lesioned spinal cord and observed robust axon growth as well as motor recovery (Lu et al., 2012). These

Received July 4, 2013; revised Sept. 18, 2013; accepted Sept. 24, 2013.

Author contributions: S.H. and A.B. designed research; S.H., L.G., and P.L. performed research; V.J.T. contributed unpublished reagents/analytic tools; S.H., P.L., and A.B. analyzed data; S.H., P.L., and A.B. wrote the paper.

This work was supported by National Institutes of Health/National Institute of Neurological Disorders and Stroke Grant NS054883, Wings for Life, International Foundation for Research in Paraplegia, and International Spinal Research Trust (all to A.B.), Craig H. Neilsen Foundation Grant 161456 (postdoctoral fellowship; S.H.), and the Veterans Administration and Canadian Spinal Research Organization (P.L.). We thank the Rat Resource and Research Center, University of Missouri (Columbia, MO) for providing GFP rats.

Correspondence should be addressed to either of the following: Dr. Armin Blesch, Spinal Cord Injury Center, Heidelberg University Hospital, Schlierbacher Landstrasse 200a, D-69118 Heidelberg, Germany, E-mail: armin.blesch@med.uni-heidelberg.de; or Dr. Paul Lu, Center for Neural Repair, Department of Neurosciences, University of California, San Diego, 9500 Gilman Drive, La Jolla, CA 92093-0626, E-mail: plu@ucsd.edu.

DOI:10.1523/JNEUROSCI.2851-13.2013

 0270-6474/13/3317138-12$15.00/0

experiments provide the basis to test the hypothesis that implantation of embryonic brainstem neurons in the lesioned spinal cord will reestablish supraspinal regulation of denervated SPNs, thereby improving cardiovascular function.

To pursue this goal, we grafted embryonic day 14 (E14) brainstem-derived neural stem cells (BS-NSCs) or SC-NSCs from GFP transgenic rats into the lesion site of T4 spinal cord transections in adult wild-type rats. Eight weeks later, grafting of BS-NSCs but not SC-NSCs resulted in full recovery of resting cardiovascular parameters, whereas both grafts alleviated colon distension-induced autonomic dysreflexia. This recovery was accompanied by graft-derived axon innervation of SPNs caudal to the injury and was dependent on innervation of grafts by descending host axons.

Materials and Methods

Animals

A total of 54 adult female Fischer 344 rats weighing 150–200 g were used. Institutional Animal Care and Use Committee and Society for Neuroscience guidelines on animal care were strictly followed to minimize the number of animals used and any potential suffering. Animals were anesthetized intraperitoneally with a combination (2 ml/kg) of ketamine (25 mg/ml; Fort Dodge Animal Health), xylazine (1.3 mg/ml; Butler), and acepromazine (0.25 mg/ml; Boehringer Ingelheim) before spinal cord surgeries, biotinylated dextran amine (BDA) injections, and implantation of telemetric transmitters into the abdominal aorta through the femoral artery. Animals were divided into groups based on transplantation of E14 BS-NSCs, E14 SC-NSCs, or spinal cord transection without transplantation as control. One set of animals grafted with BS-NSCs underwent spinal cord retransection above the graft 8 weeks after transplantation.

All animals with spinal cord transection underwent Basso–Beattie–Bresnahan (BBB) testing (Basso et al., 1995) to evaluate hindlimb function 2 weeks after lesion before cell transplantation. Animals were considered potentially incompletely lesioned when the BBB score for hindlimb movements was >1. These animals were immediately excluded ($n = 6$), and only animals with scores ≤1 were grafted or included as injury controls. During histological examination, animals with an incomplete lesion identified by immunolabeling for glial fibrillary acidic protein (GFAP) in the lesion site in injury controls and GFAP-expressing ($GFAP^+$) cells within GFP-negative areas in the lesion were eliminated ($n = 1$). In a few cases, graft integration in the lesion site was poor without axon extension into the host spinal cord. Those animals were also excluded regardless of their cardiovascular measures (BS-NSC graft, $n = 2$; BS-NSC graft followed by retransection, $n = 2$; SC-NSC graft, $n = 1$). A final number of 42 rats was used for histological and cardiovascular analysis (BS-NSC graft, $n = 16$, $n = 11$ of 16 used for cardiovascular analysis, $n = 5$ of 16 used for cardiovascular analysis and retransection; SC-NSC graft, $n = 9$, $n = 6$ of 9 randomly chosen animals used for cardiovascular analysis; injury controls, $n = 11$, $n = 8$ of 11 randomly chosen animals used for cardiovascular analysis; naive rats, $n = 6$ used to assess normal cardiovascular parameters). The remaining animals and those used for cardiovascular analysis without retransection were used for histological analysis. We did not investigate sensorimotor recovery in the present study because a catheter connected to a telemetric transmitter was implanted through the femoral artery to monitor mean arterial pressure (MAP) and heart rate (HR). This can partially block blood flow to one of the hindlimbs and could influence motor behavior.

Spinal cord surgery and cell grafting

Complete T4 transection. All animals underwent a T3 dorsal laminectomy, and the dura was cut longitudinally and retracted. A 1 mm rostrocaudal piece of spinal cord at the T4 level was cut and removed using a combination of iridectomy scissors and microaspiration, with visual verification to ensure complete transection ventrally and laterally. After lesions were complete, muscles were sutured with 3-0 Vycril (Ethicon), and the skin was closed with wound clips (Roboz). Animals were administered 3 ml of lactated Ringer's solution (Baxter Healthcare) subcutaneously immediately after surgery, and ampicillin (33 mg/kg) was delivered prophylactically once daily for up to 10 d. Banamine (0.035 mg/kg; Reckitt Benckiser) was also administered subcutaneously once after recovery from anesthesia and twice daily for the next 3 d to control postoperative pain. Bladders were manually expressed twice daily until an automatic bladder-emptying reflex developed at ~10 d after injury.

BBB testing. One day before E14 cell grafting, hindlimb motor function was evaluated according to the 21-point BBB scale in an open field (Basso et al., 1995). Only animals scored 0–1 were considered to have complete spinal transection and were used for additional treatments. After perfusion, complete transection of the spinal cord was further verified histologically.

E14 BS-NSC and SC-NSC transplantation. Most supraspinal neurons regulating sympathetic activity are located at the brainstem. To determine whether reinnervation of denervated SPNs by neurons from higher autonomic centers can reconstruct neuronal circuits and improve sympathetic function, we grafted E14 BS-NSCs into the injured spinal cord, whereas SC-NSCs lacking supraspinal neurons served as a cellular control. E14 brainstem and spinal cord from transgenic Fischer 344 transgenic (EGFP) rats ubiquitously expressing GFP under the ubiquitin C promoter provided donor tissue for grafting (Rat Resource and Research Center, University of Missouri, Columbia, Missouri). At this stage, embryonic grafts are composed of a mixture of NSCs, neuronal restricted precursors, and glial restricted precursors (Kalyani and Rao, 1998). Previous studies indicated a better cellular survival when transplantation was delayed by 2 weeks after injury compared with acute grafting (Lu et al., 2012). Therefore, the spinal cord lesion site was reexposed 2 weeks after T4 transection. GFP-expressing E14 brainstem or spinal cord was freshly dissected and dissociated according to the method of Harris et al. (2007). Dissociated E14 NSCs were resuspended in a fibrin matrix (25 mg/ml fibrinogen and 25 U/ml thrombin) containing growth factors to support graft survival as described previously (Willerth et al., 2007; Grumbles et al., 2009; Lu et al., 2012): BDNF (50 μg/ml), neurotrophin-3 (50 μg/ml), platelet-derived growth factor-AA (10 μg/ml), insulin-like growth factor 1 (10 μg/ml), epidermal growth factor (10 μg/ml), basic fibroblast growth factor (10 μg/ml), glial cell line-derived neurotrophic factor (10 μg/ml), and hepatocyte growth factor (10 μg/ml). The dura was kept closed to retain cells in the lesion site. E14 cells were injected into the lesion cavity and 1 mm rostral and 1 mm caudal to the lesion center using a pulled glass micropipette with an inner diameter of 40 μm, connected to a PicoSpritzer II (General Valve). A total of 10 μl of the E14 GFP-expressing cells ($3.5 \times 10^5/\mu l$) were microinjected per rat. Animals survived for an additional 8 weeks.

BDA injection into the rostroventrolateral medulla

The five main supraspinal regions providing input to SPNs in the thoracolumbar spinal cord include the following: (1) the rostroventrolateral medulla; (2) the rostral ventromedial medulla; (3) the caudal raphe nuclei; (4) the A5 region; and (5) the paraventricular nucleus of the hypothalamus (Llewellyn-Smith, 2009). Among these autonomic centers, the rostroventrolateral medulla is considered to play a key role in regulating cardiovascular function (Schramm et al., 1993; Dampney et al., 2000). Because of the diffuse distribution of sympathetic brainstem nuclei, we chose the rostroventrolateral medulla as one representative nucleus to investigate host supraspinal axon regeneration (Hou et al., 2013). Descending vasomotor pathways were anterogradely labeled by injection of BDA (10% in distilled H_2O, molecular weight 10,000; Invitrogen) bilaterally into the rostroventrolateral medulla 5 weeks after cell grafting (3 weeks before perfusion) at two sites per side (relative to bregma: rostrocaudal −11.80 mm, mediolateral ±2.3 mm, dorsoventral 7.6 mm; rostrocaudal −12.30 mm, mediolateral ±2.2 mm; dorsoventral 7.4 mm; $n = 6$ in BS-NSC and $n = 6$ in SC-NSC). After the skull was opened using a drill, a total of 1 μl/site was injected slowly with a PicoSpritzer (General Valve). Banamine (0.035 mg/kg; Reckitt Benckiser) was administered subcutaneously after recovery from anesthesia and once daily for the next 3 d to control postoperative pain.

Fluorogold labeling

One week before perfusion, animals received an intraperitoneal injection of Fluorogold (FG; 0.4 ml of 0.5% in distill water; Fluorochrome) to label SPNs in the intermediolateral cell column (IML; Akhavan et al., 2006).

Implantation of telemetry device

Eight weeks after E14 cell transplantation (10 weeks after injury), rats were reanesthetized for instrumentation with radio telemetric pressure transducers (model TA11PA-C40; Data Sciences International) as described previously (Nout et al., 2012; Hou et al., 2013). A skin incision was made on the ventral abdomen and the inner thigh region on the right side to expose the femoral vessels. The artery was separated from the femoral vein and nerve. One milliliter of lidocaine (2%) was applied to the surface of the artery to elicit diastolization. After securing the vessel distally and temporary blocking proximally, the artery was punctured and the tip of the catheter (8 cm long) was inserted using a catheter insertion tool (20 gauge curved needle). The catheter was advanced rostrally so that the tip was placed in the abdominal aorta. Once the catheter was anchored in the vessel, a subcutaneous pocket along the flank was made between the caudal edge of the ribcage and the most cranial extension of the range of motion of the keen with a blunt scissors. The transmitter body was inserted into the pocket, and the surrounding tissue at the end of transmitter was sutured to avoid any movement. The skin was closed with surgical staples.

Basal cardiovascular parameters for recording and analyses

The Dataquest acquisition and analysis system ART (Data Sciences International) was used for telemetric monitoring of hemodynamic parameters. Data collections were performed in two phases: (1) at least 1 h for the resting parameters; and (2) 3 min for colorectal distension-induced cardiovascular parameters. On the day after transmitter implantation, the device was turned on and the cage with a single animal was put on the top of the receiver for ~10–15 min to habituate the animal and to stabilize the cardiovascular curve. During this time, pulse arterial pressure was transmitted as a radiofrequency signal to a receiver, and data from receivers were collected and analyzed. MAP and HR values were derived from the pulse arterial pressure with a computerized acquisition system. For each animal, data collected every 5 s were averaged for up to 1 h resting recording, whereas data were sampled every 3 s for 3 min colorectal distension-induced recording.

Colorectal distension and autonomic dysreflexia

To initiate spinal viscero-sympathetic reflexes, 2–3 d after transmitter transplantation, a latex balloon-tipped catheter (Swan-Ganz; Edwards LifeSciences) was inserted for ~2 cm into the rectum and secured to the tail with tape (Maiorov et al., 1997, 1998). Animals usually did not show any signs of distress to the presence of the catheter within the distal portion of the large intestine. After 10–15 min stabilization, colorectal distension was induced by inflation of the balloon with 1.4 ml of air for 1 min. This volume of air generated a pressure of ~30 mmHg. At least two distensions with a 0.5–1 h recovery period were implemented in a quiet environment. Parameters were measured before (baseline), during, and after a 1 min period of balloon catheter inflation. An animal was regarded as dysreflexic if colorectal distension produced a rise in MAP and a decrease in HR (Krenz and Weaver, 1998; Maiorov et al., 1998; Inskip et al., 2009). For each animal, the difference between baseline MAP and colorectal distension-induced MAP change was calculated for each trial and then averaged over the two trials.

Tissue processing and immunohistochemistry

Animals were overdosed with an anesthesia mixture and perfused transcardially with 0.1 M PBS, pH 7.4, followed by 4% paraformaldehyde in PBS. Spinal cords were dissected, postfixed overnight, and cryoprotected in 30% sucrose in 0.1 M Tris-buffered saline (TBS). A piece of spinal cord spanning 0.5 cm rostral and 2.5 cm caudal to the lesion site (approximate levels T2–T10) was embedded in gum tragacanth (Sigma-Aldrich) in 30% sucrose/PBS for cryosectioning, as described previously (Cameron et al., 2006). Spinal cords were serially sectioned in the longitudinal, horizontal plane at 35 μm in six series of free-floating sections.

Free-floating sections were incubated with primary antibodies against GFP [rabbit, 1:1500 (Invitrogen); goat, 1:1500 (Millipore Bioscience Research Reagents)] to label GFP-expressing embryonic cells, GFAP [mouse, 1:1500 (Millipore Bioscience Research Reagents); rabbit, 1:1500 (Dako)] to label astrocytes, NeuN (mouse, 1:200; Millipore Bioscience Research Reagents) to label mature neurons, 5-HT (rabbit, 1:20,000; Immunostar) to label serotonergic neurons and axons; tyrosine hydroxylase (TH; mouse, 1:1000; Millipore Bioscience Research Reagents) to label catecholaminergic neurons and axons, and synaptophysin (mouse, 1:1000; Millipore Bioscience Research Reagents) to label presynaptic terminals. Sections were incubated in primary antibody solution overnight at 4°C and then incubated in Alexa Fluor 488-, 594-, or 647-conjugated goat or donkey secondary antibodies (1:250; Invitrogen) for 2.5 h at room temperature. To label BDA^+ fibers for light-level microscopy, endogenous peroxidase activity was blocked with 0.6% hydrogen peroxide in TBS for 15 min. After washing for three times, sections were incubated in avidin-biotinylated peroxidase complex (Elite kit; 1:100; Vector Laboratories) for 6 h at room temperature. Diaminobenzidine (0.05%) with nickel chloride (0.04%) was used as chromagen, with reactions sustained for 0.5–10 min. For fluorescent labeling, sections were incubated in Alexa Fluor 594-conjugated streptavidin (1:250) overnight at 4°C. Photographs were taken using a MicroFire digital camera (Optronics) connected to an Olympus AX-70 microscope. For confocal imaging, an Olympus Fluoview 1000 microscope was used.

Quantification of immunolabeling

All quantifications for histological analysis were conducted by an observer blinded to group identity.

GFAP expression. The density of GFAP immunolabeling was measured at 100× magnification using NIH ImageJ. Two sections containing IML and one section containing the central canal were quantified in one series. In animals with grafts, measurements were made at the caudal host/graft interface. In animals without graft, GFAP labeling density was quantified in the caudal spinal cord stump. Individual values from each animal were averaged and used for statistical comparison.

TH^+/5-HT^+ cells and axons. To determine the number of TH^+/5-HT^+ cells in the graft, one of six serial 35 μm horizontal longitudinal thoracic spinal cord sections triple labeled for TH or 5-HT, GFP, and GFAP were examined under fluorescence microscopy. TH^+/5-HT^+ cells were counted at 100× magnification in two sections containing the IML region and one section containing the central canal in each animal. Only cells displaying a neuronal profile with cellular processes were counted. The total number of labeled neurons in all three sections was used for statistical analysis.

The density of TH/5-HT-immunolabeled fibers in the IML region was measured using NIH ImageJ in two sections containing the IML region per animal. To standardize the region of interest for every animal, we selected three IML regions in each section in which the most densely labeled fibers associated with FG-labeled SPNs were visible. Grayscale photographs were acquired at 400× magnification using epifluorescent illumination and appropriate wavelength filters. The density of fibers was quantified in this area. Thresholding values on images were chosen such that only TH^+/5-HT^+-immunolabeled axons were measured. Nonspecific staining or labeling artifacts were edited from images. For each animal, total labeled pixels were obtained by summing labeled pixels on two individual sections, as well as total photographed area. Axon density was determined by dividing the total number of labeled pixels by the total photographed area used for quantification. The distance of longest TH^+/5-HT^+ axons in the IML were also calculated using a calibrated eyepiece with a scale at 200× magnification.

BDA-labeled rostroventrolateral medulla-derived axons. Two sections containing the IML and one section containing the central canal were quantified in one series of sections per animal. BDA-labeled axonal profiles, labeled for light microscopy, within the GFP^+ BS-NSC or SC-NSC grafts were counted at 200× magnification. The total number of BDA-labeled axonal profiles in all three sections was used for statistical analysis.

Statistics

All cardiovascular responses (at least two trials) per rat were averaged. Data of hemodynamics and histology including GFAP expression density in graft/lesion site and the amount of BDA-labeled medullary descending axons were compared by ANOVA with Fisher's PLSD. A significance criterion of $p < 0.05$ was used. A nonparametric Kruskal–Wallis test followed by Mann-Whitney U tests were used to analyze TH^+ and

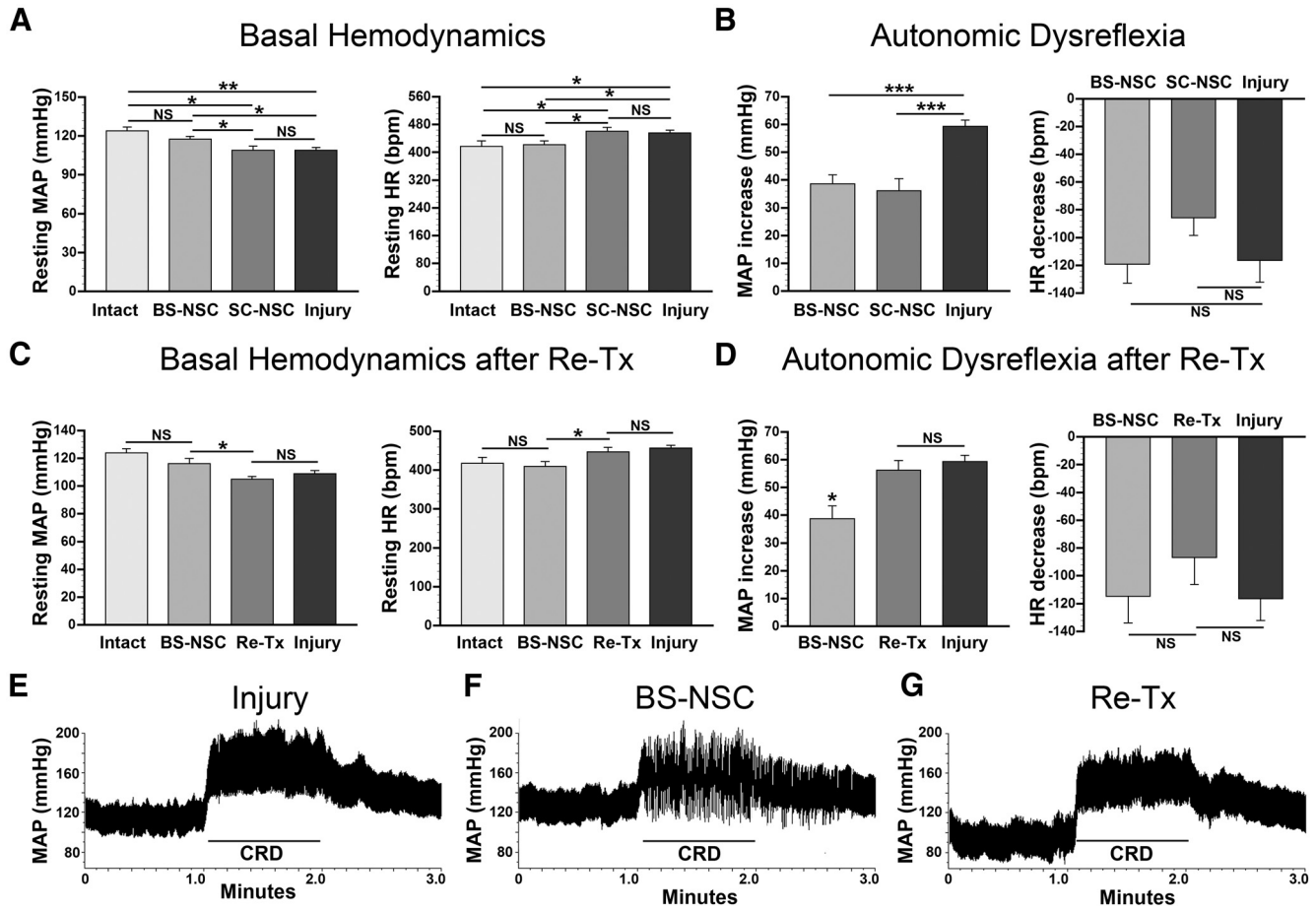

Figure 1. Analysis of basal cardiovascular parameters and colorectal distension (CRD)-induced autonomic dysreflexia. ***A***, Ten weeks after complete T4 transection, significantly lower (ANOVA, $p = 0.002$; Fisher's PLSD, $^{**}p < 0.01$) resting MAP and higher (ANOVA, $p = 0.02$; Fisher's PLSD, $^{*}p < 0.05$) resting HR are evident in control animals that received only an injury compared with intact animals. Resting MAP and HR are restored to virtually normal levels (Fisher's PLSD, both $^{*}p < 0.05$ compared with injury-only controls) in BS-NSC-grafted animals, whereas parameters in animals implanted with SC-NSCs do not significantly (Fisher's PLSD, MAP, $p = 0.98$; HR, $p = 0.78$) recover. ***B***, CRD-induced autonomic dysreflexia is evident in all animals. However, the magnitude of MAP increases during CRD is smaller in animals grafted with BS-NSCs and SC-NSCs than those in the injury-only group (ANOVA, $p < 0.001$; Fisher's PLSD, $^{***}p < 0.001$). No differences in the changes of HR were evident between groups. ***C***, After spinal cord retransection (Re-Tx) above the level of BS-NSC grafts, resting MAP is significantly (paired *t* test, $p < 0.05$) reduced and HR is increased (paired *t* test, $p < 0.05$), reaching the levels of injury-only controls animals. ***D***, Retransection also causes significantly (paired *t* test, $p < 0.05$) more exaggerated MAP increases after CRD, whereas HR remains unaffected. ***E–G***, Representative examples of MAP recordings before, during, and after CRD. A dramatic rise in MAP can be seen in animals that received only an injury when a balloon-tipped catheter is inflated in the colon (***E***). Notably, the extent of MAP increase is smaller during CRD in an animal grafted with BS-NSCs in the lesion site (***F***). After a subsequent retransection above the lesion in the same animal (***G***), MAP increases are amplified after noxious stimulation to a similar level as observed in injury-only control animals.

5-HT^{+} neuron number, axon density, and axon extension. For retransection experiments, paired *t* tests were used to compare HR and MAP before and after spinal retransections with a significance criterion of $p < 0.05$. All values are expressed as the mean ± SEM.

Results

Adult Fischer 344 rats underwent T4 complete spinal cord transection. Two weeks later, embryonic BS-NSCs or SC-NSCs from inbred Fischer 344 GFP transgenic rats were grafted to the lesion site of T4 complete spinal cord transections. Animals survived an additional 8 weeks. Using a telemetric system with transducers implanted into the aorta, resting MAP and HR were recorded. Autonomic dysreflexia was elicited by unpleasant colorectal distension. Selected animals underwent spinal cord retransection above the graft, and cardiovascular parameters and responses were analyzed. To anterogradely trace host supraspinal vasomotor pathways, BDA was delivered bilaterally into the rostroventrolateral medulla of the brainstem 3 weeks before perfusion. FG was injected intraperitoneally to retrograde label SPNs in the spinal cord 1 week before the animals were killed.

BS-NSC grafting restores basal MAP and HR

Supraspinal vasomotor pathways regulate the tonic activity of SPNs to maintain basal hemodynamics, and the loss of bulbospinal control results in low basal sympathetic tone (Stjernberg et al., 1986; Maiorov et al., 1997). Rats with complete SCIs usually develop long-lasting hypotension at rest and compensatory tachycardia attributable to baroreflex-mediated responses (Laird et al., 2006).

We recorded basal MAP and HR 1 d after implantation of a telemetric transducer into the aorta through the femoral artery, 10 weeks after lesion, once hemodynamics were stable. In animals with injury alone ($n = 8$), MAP was significantly (ANOVA, $p < 0.05$, Fisher's PLSD; $p < 0.01$) reduced (109 ± 2 mmHg) whereas HR increased (457 ± 8 bpm; ANOVA, $p < 0.05$; Fisher's PLSD, $p < 0.05$) compared with naive animals (MAP, 124 ± 3 mmHg; HR, 418 ± 16 bpm; $n = 6$; Fig. 1*A*), consistent with previous reports (Laird et al., 2006). After BS-NSC grafting ($n = 11$), both MAP and HR approached levels measured in naive animals (MAP, 118 ± 2 mmHg; HR, 422 ± 11 bpm) and were significantly different from injured control animals without graft (Fish-

er's PLSD, both $p < 0.05$; Fig. 1*A*). In contrast, MAP and HR did not show any significant changes in animals grafted with SC-NSCs (MAP, 109 ± 3 mmHg; Fisher's PLSD, $p = 0.98$; HR, 462 ± 11 bpm; Fisher's PLSD, $p = 0.78$; $n = 6$) compared with animals with injury alone (Fig. 1*A*). Thus, basal hemodynamics can be virtually normalized by BS-NSC but not by SC-NSC implantation after high thoracic SCI.

BS-NSC grafting mitigates autonomic dysreflexia

To investigate potential changes in autonomic dysreflexia after transplantation, a balloon-tipped catheter was inserted into the rectum 8 weeks after transplantation. Colorectal distension was implemented in all animals using a balloon inflated with 1.4 ml of air (exerting a pressure of ~30 mmHg). The most frequently measured hemodynamic components MAP and HR were recorded before, during, and after colorectal distension. Dysreflexic hypertension and bradycardia were inevitably triggered in all animals, but the extent differed between groups. In animals with injury alone ($n = 6$), MAP increased by 59.3 ± 2.3 mmHg during colorectal distension with small variability among rats (Fig. 1*B*). Markedly, the increase in MAP in animals grafted with BS-NSCs ($n = 7$) was only 38.6 ± 3.3 mmHg, which was significantly (ANOVA, $p < 0.001$; Fisher's PLSD, $p < 0.001$) less compared with injured control animals without graft. Colorectal distension-induced hypertension was also smaller in animals implanted with SC-NSCs (increase by 36.1 ± 4.5 mmHg; $n = 6$; Fisher's PLSD, $p < 0.001$). Unlike the partially alleviated hypertension, the decrease in HR during the period of colorectal distension did not significantly (ANOVA, $p > 0.05$) differ between groups, although the bradycardia was less severe in both grafted groups (Fig. 1*B*).

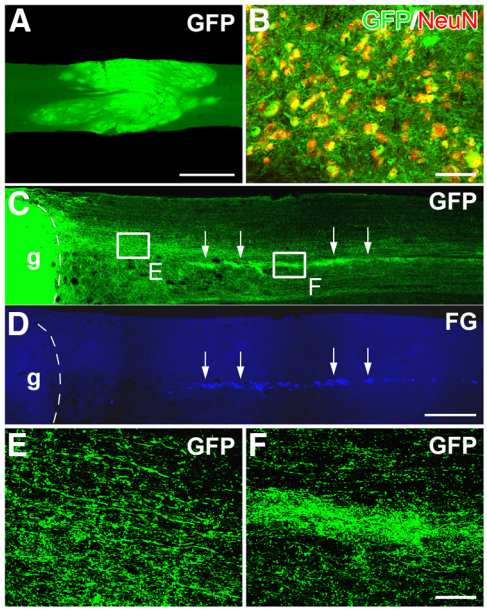

Figure 2. BS-NSCs integrate in the host spinal cord and show robust axon growth projecting to the caudal IML. ***A***, The spinal cord lesion site is filled with GFP-expressing BS-NSCs. Grafted cells reconnect the rostral and caudal spinal stumps. ***B***, Some GFP $^+$ cells colocalize with the mature neuronal marker NeuN, indicating maturation of BS-NSCs into adult neurons in the host spinal cord. ***C–F***, Numerous axons emerge from BS-NSC grafts into the caudal white and gray matter over remarkable distance (***C***). Notably, denser GFP $^+$ axons are located in the IML identified by retrograde labeling with FG (***D***; arrows in ***C***, ***D***). Higher magnification of dense GFP $^+$ axons in the white matter (***E***) near the graft (g) and in the caudal IML (***F***). Scale bars: ***A***, 1 mm; ***C***, ***D***, 0.5 mm; ***B***, ***E***, ***F***, 50 μm.

Retransection abolishes cardiovascular functional recovery

To determine whether the partial recovery of cardiovascular function in BS-NSC-grafted animals was attributable to supraspinal control or solely to BS-NSC-mediated reinnervation or neuroprotection, spinal cords were retransected rostral to the implant in randomly selected animals grafted with BS-NSCs ($n = 5$) after basal hemodynamics and colorectal distension-induced autonomic dysreflexia were recorded 8 weeks after grafting. In this cohort of animals, BS-NSC grafting also resulted in the normalization of basal MAP and HR (MAP, 116 ± 4 mmHg; HR, 410 ± 13 bpm) and a reduction of MAP increases (38.6 ± 4.6 mmHg) after colorectal distension compared with controls. Importantly, after spinal cord retransection above the graft, the graft-mediated normalization of basal MAP and HR was completely abolished (paired *t* test, both $p < 0.05$), returning to levels observed in animals without graft. Resting MAP decreased to 105 ± 2 mmHg and HR increased to 447 ± 10 bpm (Fig. 1*C*). In addition, the magnitude of MAP rises during colorectal distension-induced autonomic dysreflexia increased by 46% to 56.3 ± 3.4 mmHg after retransection (Fig. 1*D–G*), a value that was not significantly different

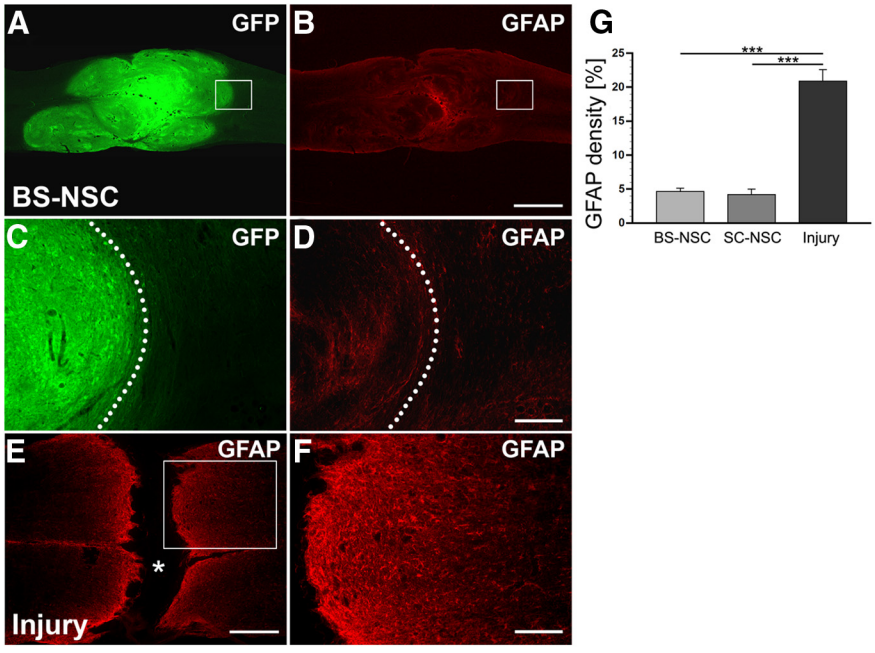

Figure 3. Grafted BS-NSCs survive and integrate in the host parenchyma, reducing injury-induced astrogliosis. ***A–D***, The lesion site at level T4 is completely filled with GFP-labeled implanted BS-NSCs. Grafted cells integrate in the rostral and caudal host spinal cord. GFAP expression is low in BS-NSC grafts and the surrounding host spinal cord. At higher magnification (***D***), weak GFAP labeling can be observed at the host/graft interface identified by GFP immunolabeling (***C***, dotted lines). ***E***, ***F***, In the spinal cord of animals that received no graft, a lack of GFAP labeling in the lesion site (asterisk) and an upregulation of GFAP in spinal parenchyma adjacent to the lesion site representing the glial scar is visible. Boxed regions in ***A***, ***B***, and ***E*** are shown at higher magnification in ***C***, ***D***, and ***F***, respectively. ***G***, Compared with animals that received an injury but no graft, the density of GFAP immunolabeling at the lesion border is significantly lower in animals grafted with BS-NSCs or SC-NSCs (ANOVA, $p < 0.0001$ with Fisher's PLSD, ***$p <$ 0.0001). Scale bars: ***A***, ***B***, 1 mm; ***C***, ***D***, ***F***, 200 μm; ***E***, 0.5 mm.

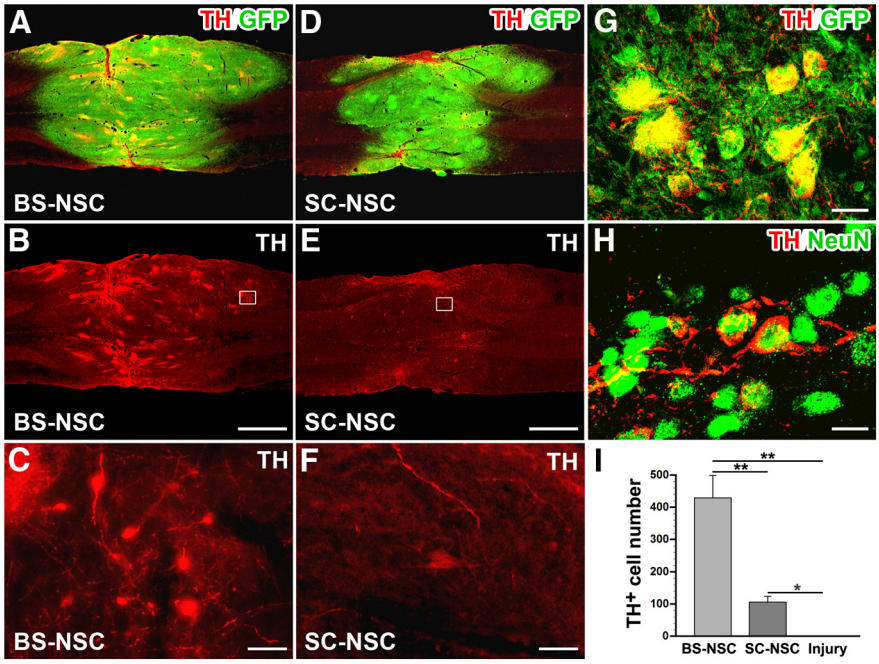

Figure 4. Differentiation of catecholaminergic neurons from NSC implants. ***A***, ***B***, Eight weeks after transplantation, immunolabeling for TH (red) and GFP (green) reveals numerous TH$^+$ neurons and fibers within BS-NSC implants in a horizontal spinal cord section. ***C***, TH$^+$ neurons often cluster in the graft. ***D–F***, Much fewer, scattered TH-labeled cells are found in SC-NSC grafts. Boxed regions in ***B*** and ***E*** are shown at higher magnification in ***C*** and ***F***. ***G***, ***H***, Embryonic brainstem-derived TH$^+$ cells colocalize with GFP (***G***) and the mature neuronal marker NeuN (***H***). ***I***, Quantification shows a significantly larger number of TH-labeled neurons in BS-NSC implants compared with SC-NSC grafts (Kruskal–Wallis test, $p < 0.0001$; Mann–Whitney *U* test, $^{**}p < 0.001$). The number of TH-labeled neurons in SC-NSC implants is also significantly different from injury-only controls (Mann–Whitney *U* test, $^{*}p < 0.01$). Scale bars: ***A***, ***B***, ***D***, ***E***, 1 mm; ***C***, ***F***, 25 μm; ***G***, 10 μm; ***H***, 12.5 μm.

from the increase observed in injured control animals. Consistent with the limited effects of BS-NSC grafts on HR in the first set of experiments, interrupting descending supraspinal projections by retransection did not result in dramatic changes in HR.

Thus, spinal cord retransection abolishes hemodynamic recovery, suggesting that cardiovascular parameters are influenced by inputs from neurons above the graft.

Integrated grafts display remarkable axon extension and topographical axon innervation

After recording of hemodynamic parameters 8 weeks after embryonic NSC transplantation, spinal cords were processed for histological analysis. In spinal cords implanted with BS-NSCs or SC-NSCs, GFP immunolabeling demonstrated excellent graft survival. Embryonic NSCs completely filled the lesion site, and only minor cavities or gaps were observed. Implants integrated into the host gray and white matter both rostrally and caudally (Figs. 2*A*, 3*A*,*C*). Consistent with our previous findings, some GFP$^+$ cells were detected in the rostral and caudal stumps as a result of multiple cell injection sites. Numerous GFP-labeled cells in the graft colocalized with the mature neuronal marker NeuN (Fig. 2*B*).

In all injured control animals without graft, a dense glial scar was evident at the rostral and caudal spinal cord stumps (Fig. 3*E*,*F*). In contrast, the majority of animals grafted with BS-NSCs (Fig. 3*A–D*) or SC-NSCs (data not shown) showed very limited injury-induced upregulation of GFAP immunolabeling at the host/graft interface and little GFAP immunoreactivity within BS-NSC/SC-NSC implants (Fig. 3*B*,*D*). Quantification of GFAP density in randomly selected animals at the host/graft interface and spinal cord stumps, respectively, demonstrated significantly lower GFAP expression in spinal cords grafted with BS-NSCs ($n = 10$) and SC-NSCs ($n = 9$; ANOVA, $p < 0.0001$; Fisher's PLSD, $p < 0.0001$) compared with injured control animals without graft ($n = 9$; Fig. 3*G*). Therefore, grafted BS-NSCs and SC-NSCs survive and integrate into the host spinal cord. NSC grafts limit the formation of a glial scar, thereby generating a local environment favorable for axonal growth.

Grafted BS-NSCs or SC-NSCs extended a large number of axons into the host spinal cord in both rostral and caudal direction over remarkable long distances (Fig. 2*C*). Emerging GFP$^+$ processes colabeled with the axonal marker neurofilament (data not shown). In the spinal cord caudal to the grafts, most GFP$^+$ axons grew in white matter and some crossed into the gray matter (Fig. 2*C*,*E*). Strikingly, a large number of BS-NSC-derived axons projected to the IML, in which FG-labeled SPNs are located (Fig. 2*C*,*D*). The topographical innervation along the IML, indicated by very dense GFP$^+$ axons (Fig. 2*C*,*F*), was evident in BS-NSC-grafted but not in SC-NSC-grafted spinal cords. Eight weeks after implantation, GFP$^+$ axons extended for >20 mm in the IML region in many cases ($n = 6$ of 10 in BS-NSC, $n = 4$ of 9 in SC-NSC) covering more than seven spinal segments.

Graft-derived catecholaminergic neurons project to the IML

In the intact spinal cord, SPNs in the IML receive catecholaminergic input primarily from C1 adrenergic and A1/A5 noradrenergic neurons in the brainstem to regulate cardiovascular dynamics (Sawchenko and Bohn, 1989; Bruinstroop et al., 2012). Loss of adrenergic and noradrenergic input is a major factor underlying sympathetic disorders after SCI. Eight weeks after BS-NSC grafting, TH immunolabeling revealed a large number of catecholaminergic cells and fibers within the implants (Fig. 4*A–C*). TH$^+$ cells were often encountered as cell clusters and fiber patches without specific spatial distribution in the implants. Colocalization of TH and GFP clearly indicated their origin from embryonic implants and not from host tissue (Fig. 4*G*). Embryonic brainstem-derived TH$^+$ cells also expressed the mature neuronal marker NeuN (Fig. 4*H*), indicating maturation to an adult phenotype in the graft within 8 weeks. In contrast, very few faint TH-immunolabeled cells were present in SC-NSC implants and only a few individual axons (Fig. 4*D–F*). In injured animals without implant, TH immunolabeling did not reveal any labeled profiles within the lesion site. Quantitative analysis showed significantly more TH$^+$ cells in BS-NSC implants compared with animals transplanted with SC-NSCs (Kruskal–Wallis test, $p < 0.0001$; Mann–Whitney *U* test, $p < 0.001$). TH$^+$ cell number in SC-NSC grafts was approximately fourfold lower but still significantly different from injured control animals ($p < 0.01$; Fig. 4*I*).

In animals grafted with BS-NSCs, TH-immunolabeled fibers originating from the implant extended caudally in white and gray matter. Notably, numerous TH$^+$ fibers were fasciculated and projected along the IML, in close association with FG-labeled SPNs (Fig. 5*A–D*). In most cases, TH-labeled axon bundles in the IML extended for several spinal segments. In contrast, TH$^+$ fi-

bers were rarely detected below the implant in animals that received SC-NSC implants, and only occasional TH-labeled axons within a short distance were observed in the IML region, consistent with the small number of TH^+ cells within SC-NSC grafts (Fig. 5*E–H*). In injured animals without graft, catecholaminergic fibers were not observed in thoracolumbar white or gray matter below the lesion (Fig. 5*I–L*). Quantification of TH^+ axon density revealed a significantly higher number (Kruskal–Wallis test, $p < 0.0001$; Mann–Whitney *U* test, $p < 0.01$) and increased growth distance (Kruskal–Wallis test, $p < 0.0001$; Mann–Whitney *U* test, $p < 0.01$) of TH-labeled fibers in the IML of spinal cords grafted with BS-NSCs than those implanted with SC-NSCs (Fig. 5*M*,*N*). In animals grafted with SC-NSCs, the number and growth distance of TH^+ axons were much lower but were still significantly different from injured control animals without graft (Mann–Whitney *U* test, $p < 0.001$). Confocal microscopy confirmed colocalization of TH-immunolabeled fibers with GFP (Fig. 5*O*) and the presynaptic marker synaptophysin in the IML (Fig. 5*P*). These data suggest that grafted embryonic catecholaminergic neurons cannot only project caudally to autonomic nuclei but also form synaptic connections, thereby contributing to the observed cardiovascular functional recovery after SCI.

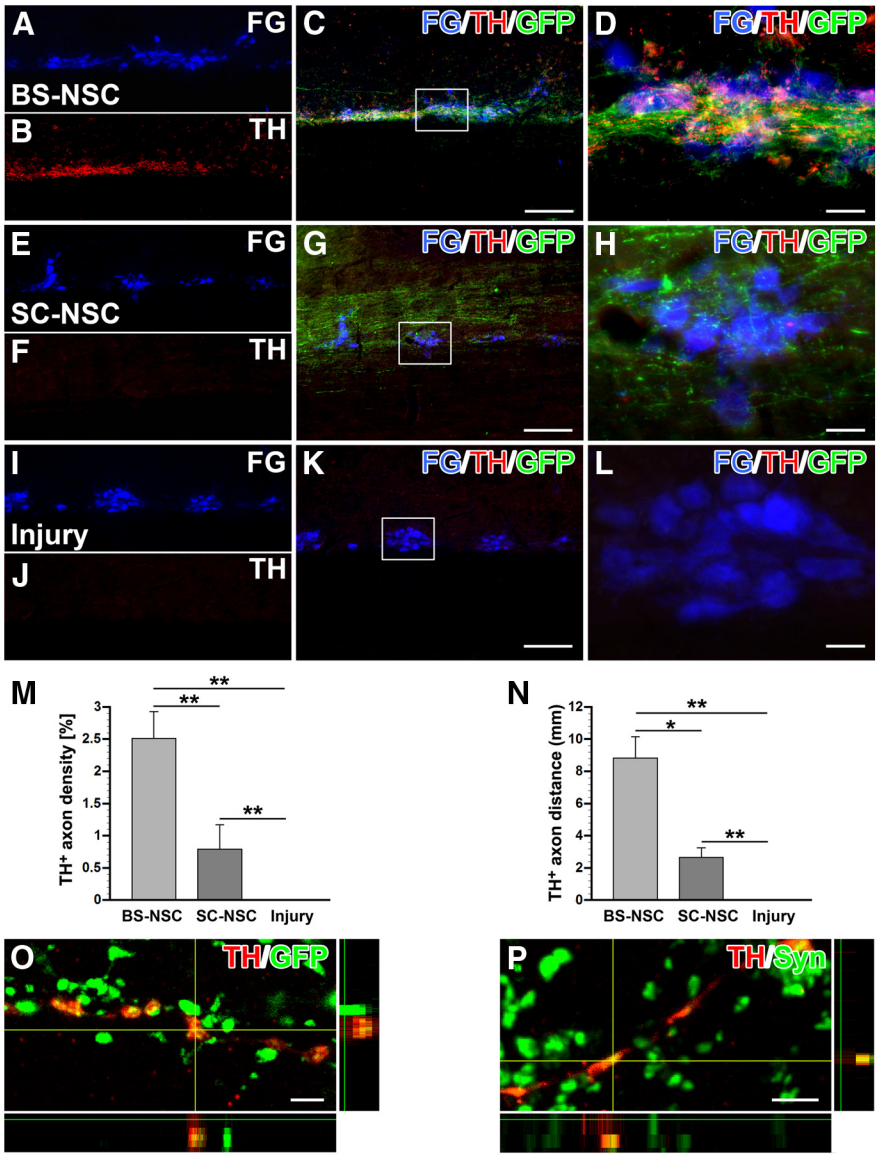

Figure 5. Catecholaminergic axons extend from BS-NSC caudally and innervate the IML. SPNs in the IML are identified by FG (***A***, ***E***, ***I***, blue). ***A–D***, TH (red) and GFP (green) double immunolabeling illustrates bundles of catecholaminergic projections that extended along the IML ~1.5 cm caudal to the injury/graft, in which they closely associate with FG-labeled SPNs. ***E–H***, In contrast, very few or no TH^+ axons are found in the IML of SC-NSC-grafted spinal cords. ***I–L***, No TH-labeled fibers are present below the lesion in animals without graft. Boxed region in ***C***, ***G***, and ***K*** are shown at higher magnification in ***D***, ***H***, and ***L***, respectively. ***M***, ***N***, Quantification of TH-labeled fibers below the lesion/graft demonstrates significantly higher density in BS-NSC-grafted animals than in SC-NSC-grafted animals (***M***; Kruskal–Wallis test, $p < 0.0001$; Mann–Whitney *U* test, $^*p < 0.01$) and injury controls ($^{**}p < 0.001$) and more extended axonal growth (***N***; Kruskal–Wallis test, $p < 0.0001$; Mann–Whitney *U* test, $^*p < 0.01$ and $^{**}p < 0.001$, respectively). TH^+ axon density ($^{**}p < 0.001$) and distance ($^{**}p < 0.001$) in SC-NSC-grafted spinal cords are also significantly different from injured control animals. ***O***, ***P***, Confocal 3D analysis shows higher magnification of TH-labeled BS-NSC-derived projections in the IML expressing GFP (***O***) and the presynaptic marker synaptophysin (***P***, Syn). Scale bars: ***A–C***, ***E–G***, ***I–K***, 200 μm; ***D***, ***H***, ***L***, 25 μm; ***O***, ***P***, 5 μm.

Graft-derived serotonergic neurons project to the IML

Caudal raphe nuclei in the brainstem are another important supraspinal center regulating spinal sympathetic function (Chalmers et al., 1988; Jansen et al., 1995). Serotonergic neurons in nucleus raphe magnus, raphe pallidus, and raphe obscurus provide input to SPNs in the spinal cord. The loss of serotonergic innervation after SCI has been reported to be one reason for disordered hemodynamics (Llewellyn-Smith et al., 2006; Cormier et al., 2010). Eight weeks after BS-NSC grafting, 5-HT immunolabeling identified many serotonergic neurons and axons within GFP^+ implants (Fig. 6*A–C*), whereas only very few scattered 5-HT^+ cells were present in SC-NSC grafts (Fig. 6*D–F*). 5-HT-labeled cells colocalized with GFP and the mature neuronal marker NeuN (Fig. 6*G*,*H*). Quantification demonstrated a significantly higher number of serotonergic neurons within BS-NSC grafts compared with SC-NSC grafts (Kruskal–Wallis test, $p < 0.0001$; Mann–Whitney *U* test, $p < 0.001$; Fig. 6*I*). No 5-HT labeling was observed in the lesion site of animals without graft.

Below the level of injury, 5-HT-labeled axon bundles emerged from BS-NSC grafts and extended along the IML, in which axons were in close contact with FG-labeled SPNs (Fig. 7*A–D*). Labeled fasciculated axons usually extended across several spinal segments. More diffuse and sparse fibers were also visible in other gray matter areas and in white matter. Unexpectedly, 5-HT-immunolabeled axons were also observed in the IML of animals with SC-NSC implants (Fig. 7*E–H*) albeit with a lower density. These serotonergic axons were probably at least partially derived from a small contamination of spinal cord implants with caudal raphe nuclei. In injured control animals without graft, no serotonergic fibers were detected caudal to the spinal cord lesion (Fig. 7*I–L*). Quantification of 5-HT^+ axons in the IML showed a sig-

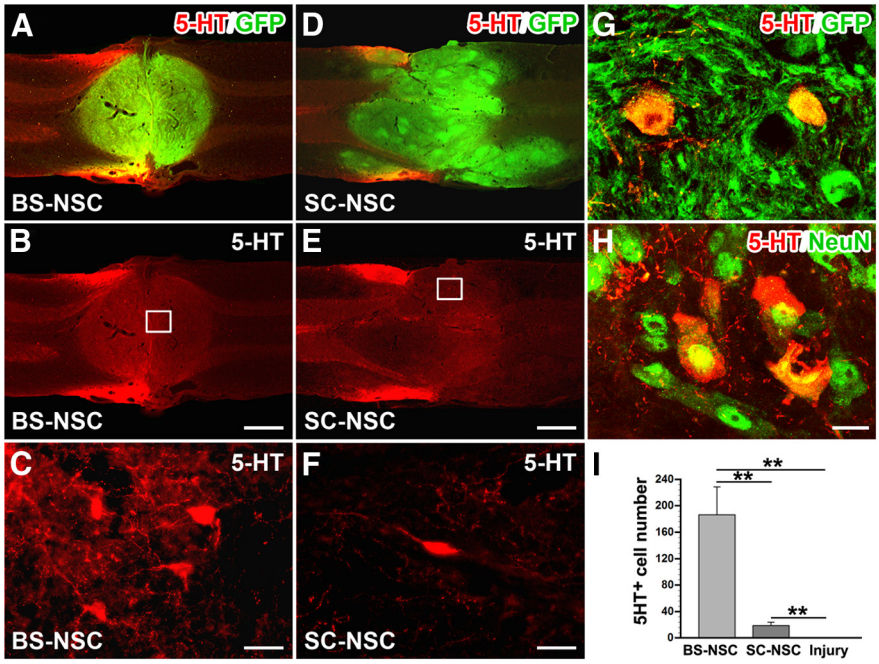

Figure 6. Differentiation of serotonergic neurons within BS-NSC implants. ***A–C***, Eight weeks after BS-NSC grafting, immunolabeling for 5-HT (red) and GFP (green) reveals many 5-HT$^+$ cells and fibers within the implant in a longitudinal thoracic spinal cord section. ***D–F***, Only occasional 5-HT$^+$ cells are found in SC-NSC implants. Boxed regions in ***B*** and ***E*** are shown at higher magnification in ***C*** and ***F***. ***G***, ***H***, 5-HT-labeled cells in BS-NSC grafts colocalize with GFP immunolabeling (***G***) and the mature neuronal marker NeuN (***H***). ***I***, Quantitative analysis indicates significantly greater number of 5-HT-immunolabeled cells in BS-NSC implants compared with SC-NSC grafts and injured control animals (Kruskal–Wallis test, $p < 0.0001$; Mann–Whitney *U* test, $^{**}p < 0.001$) and in SC-NSC grafted animals compared with injured control animals ($^{**}p < 0.001$). Scale bars: ***A***, ***B***, ***D***, ***E***, 1 mm; ***C***, ***F***, 25 μm; ***H***, 12.5 μm.

nificantly higher axon density in BS-NSC-grafted animals compared with injured control animals (Kruskal–Wallis test, $p < 0.0001$; Mann–Whitney *U* test, $p < 0.001$; Fig. 7*M*), as well as increased growth distance (Kruskal–Wallis test, $p < 0.001$, $p < 0.001$). 5-HT$^+$ axon density and the maximum distance of 5-HT$^+$ axon growth in SC-NSC-grafted spinal cords was also significantly higher than in injured control animals ($p < 0.001$ and $p < 0.01$, respectively; Fig. 7*N*). Confocal microscopy further confirmed the origination of 5-HT-labeled axons from cellular implants by colocalization with GFP (Fig. 7*O*). Labeled fibers in the IML also expressed the presynaptic marker synaptophysin (Fig. 7*P*), suggesting their connectivity with local sympathetic neurons, thereby contributing to cardiovascular functional recovery.

Besides the IML, TH- and 5-HT-immunolabeled fibers were also present in the dorsal gray commissure below BS-NSC grafts, another autonomic nucleus in the spinal cord (data not shown). In contrast, much fewer and no labeled fibers were detected in the dorsal gray commissure of animals with SC-NSC implants and injured control animals, respectively.

Host supraspinal vasomotor pathways regenerate into grafts

To trace host supraspinal vasomotor pathways, BDA was injected bilaterally into one brainstem vasomotor center, the rostroventrolateral medulla, 3 weeks before the animals were killed. Numerous BDA-labeled descending axons were detected within GFP$^+$ BS-NSC grafts and SC-NSC grafts (Fig. 8*A*,*B*). Although supraspinal projections regenerated into the BS-NSC grafts, most of the BDA-labeled projections were restricted to the rostral part of the graft, and no BDA-labeled axons extended across the graft into the distal spinal cord. Importantly, under high magnification, the terminals of BDA-labeled axons within the graft displayed numerous bouton-like structures that colocalized with the presynaptic marker synaptophysin (Fig. 8*C*,*D*), suggesting the formation of synapses with graft-derived neurons. In animals with SC-NSC grafts, BDA-labeled descending axons also regenerated into GFP$^+$ implants with a similar pattern. Quantitative analysis revealed that the number of BDA-labeled axonal profiles within BS-NSC grafts was similar to those in SC-NSC grafts ($p > 0.05$; Fig. 8*E*), indicating that BS-NSCs and SC-NSCs have a comparable ability to facilitate the regeneration of lesioned descending bulbospinal vasomotor projections. Differences in the innervation of SC-NSC and BS-NSC graft are therefore unlikely to underlie the observed differences in the recovery of basal hemodynamics.

Altogether, connections of regenerated supraspinal vasomotor axons with graft-derived neurons and connections from graft-derived neurons to sympathetic neurons below the lesion may constitute a novel neuronal relay.

Discussion

The present study demonstrates, to the best of our knowledge, for the first time improvements of cardiovascular function by reestablishing supraspinal control via graft-derived axons connecting to SPNs. Previous studies showing cardiovascular recovery in animal models of SCI were focused on tissue protection early after injury or on the prevention of sensory axon plasticity after injury (Mabon et al., 2000; Marsh et al., 2002; Cameron et al., 2006; Tang et al., 2007; Rabchevsky et al., 2012). Based on our recent studies showing extensive, long-distance axonal regeneration by grafted embryonic spinal cord NSCs in the adult lesioned CNS when supportive fibrin matrices and a growth factor mixture were applied (Lu et al., 2012), we implanted E14 BS-NSCs and SC-NSCs into the completely transected spinal cord to investigate the potential influence on cardiovascular control. BS-NSCs include brainstem progenitors for neurons regulating sympathetic activity and may reinnervate denervated SPNs to improve sympathetic function. In contrast, SC-NSCs lacking supraspinal neurons served as a cellular control.

Accordingly, we report full recovery of basal cardiovascular parameters and mitigation of colon distension-induced autonomic dysreflexia in BS-NSC-grafted but not SC-NSC-grafted animals. Histologically, grafted embryonic BS-NSCs show remarkable axon growth with topographical innervation of SPNs in the caudal IML. In addition, medullar vasomotor pathways innervate BS-NSC grafts, thereby establishing a potential neuronal relay. Thus, transplantation of NSCs from embryonic brainstem rebuilds supraspinal regulation of denervated SPNs after SCI, leading to partial restoration of cardiovascular function. This conclusion is further supported by the abolishment of cardiovascular recovery after spinal cord retransections just above the graft.

Although multiple neurotransmitter systems participate in descending control of cardiovascular homeostasis, medullary C1

adrenergic neurons, A5 noradrenergic neurons in the vasomotor center, and caudal raphe nuclei (B1–B3) play a critical role in regulating sympathetic activity of SPNs to maintain normal arterial pressure (Reis et al., 1984; Coote, 1990; Benarroch et al., 1998). Adrenaline/noradrenaline modulates the tonic discharge of SPNs to sustain sympathetic outflow within a normal range, and serotonin increases sympathetic activity to regulate cardiovascular function (Madden and Morrison, 2006; Marina et al., 2006). Previous studies have reported that abolition of most serotonergic inputs after spinal cord contusion injuries reduces resting blood pressure (Coote, 1990), and nearly all hypotension-sensitive SPNs are innervated by serotonergic fibers (Minson et al., 2002). Similarly, during experimental hypotension in intact animals, abundant varicose TH$^+$ fibers appposing hypotension-sensitive SPNs can be identified (Minson et al., 2002). Direct innervation of SPNs by adrenergic or serotonergic projections is crucial to keep stimulated pressor responses brief and of a limited magnitude when the spinal cord is intact (Bacon and Smith, 1988; Hasséssian et al., 1993).

After complete cervical and high thoracic SCI, higher autonomic centers no longer mediate efferent control of vasomotor tone. As a result, hypotension occurs as a result of reduced sympathetic activity in SPNs and subsequent low levels of plasma catecholamine. In humans with severe SCI at a high level, orthostatic hypotension during changes in postural position is frequently observed (Mathias, 2006), whereas hypotension with compensatory tachycardia at rest can be observed in rats (Laird et al., 2006).

Here, we show that catecholaminergic and serotonergic fibers densely project to the IML caudal to a complete spinal cord lesion, in which they express presynaptic markers in close contact to host neurons, suggesting the formation of functional synapses. In animals grafted with BS-NSCs, catecholaminergic fiber density in the IML below the injury/graft is much higher, and axons extend for three times the distance detected in SC-NSC-grafted animals. Similarly, the density of serotonergic fibers and axon extension is obviously higher in BS-NSC-grafted animals compared with animals that received SC-NSCs. Because sympathetic efferents for vascular control originate from multiple thoracic spinal levels, restoring appropriate inputs to SPNs across several spinal segments may be necessary for hemodynamic recovery. Consistent with the higher innervation density and the increased growth distance, resting MAP recovers in animals with BS-NSC implants whereas hypotension is sustained when SC-NSCs are grafted to the injured spinal cord. Because of intact efferent parasympathetic cardiac pathways after thoracic SCI, HR returns to a normal level after recovery of MAP. Surprisingly, we also observed some TH$^+$ and 5-HT$^+$ neurons in SC-NSC grafts albeit at a much lower level. These neurons could be derived from the few catecholaminergic and serotonergic neurons that have been described in the spinal cord (Mouchet et al., 1986; Newton and Hamill, 1988) or from a contamination by the caudal brainstem

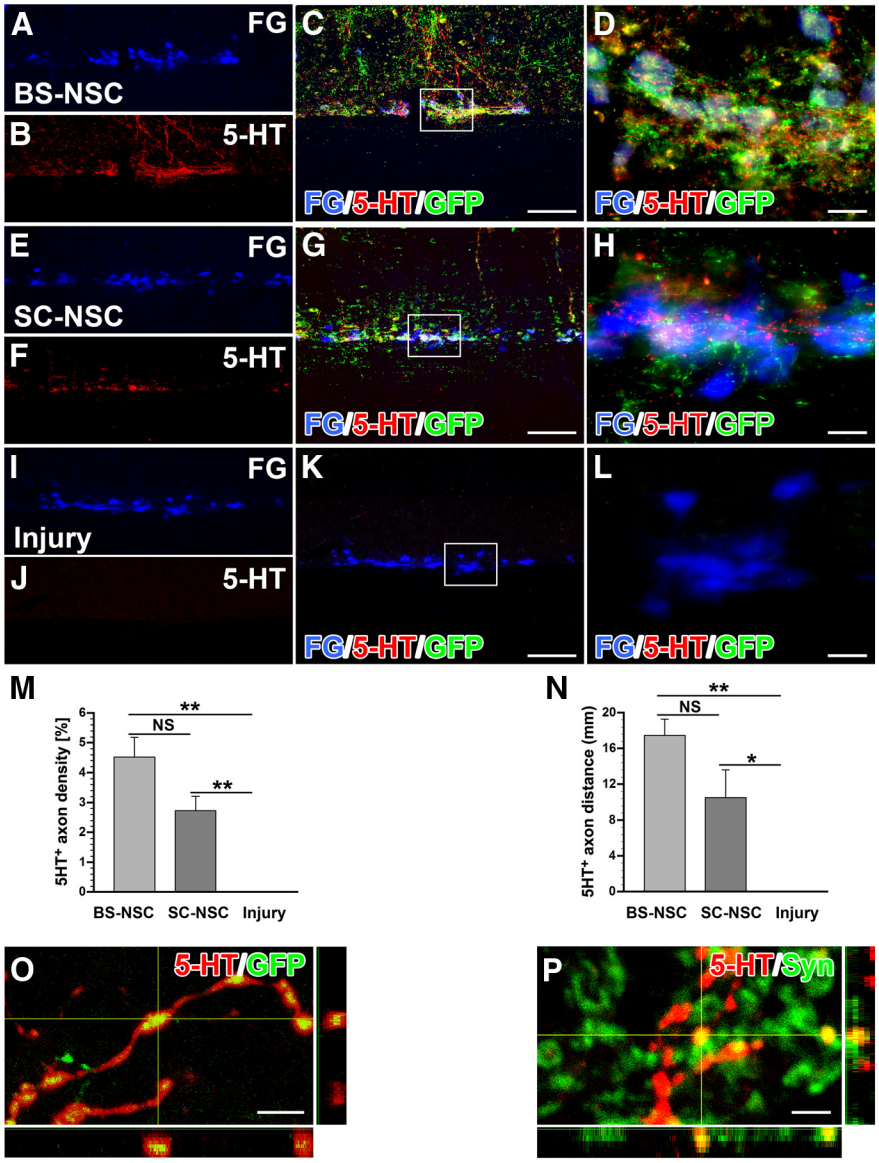

Figure 7. Serotonergic axons extend from BS-NSC grafts and innervate the IML. SPNs in the IML are identified by FG (***A***, ***E***, ***I***, blue). ***A–D***, 5-HT (red) and GFP (green) double immunolabeling illustrates bundles of serotonergic axons projecting along the IML ~1.5 cm caudal to the injury/graft site when BS-NSC are grafted into the spinal cord lesion, in which they innervate FG-labeled SPNs (***D***). ***E–H***, In animals that received SC-NSC grafts, some 5-HT-labeled axons bundles are also encountered in the IML of the thoracic spinal cord although in lower numbers. ***I–L***, No labeled fibers are present below the lesion site in injured animals without graft. Boxed region in ***C***, ***G***, and ***K*** are shown at higher magnification in ***D***, ***H***, and ***I***, respectively. ***M***, ***N***, Quantification of 5-HT-labeled fibers below the graft demonstrates a significantly higher fiber density in BS-NSC-grafted spinal cord compared with injured control animals (***M***; Kruskal–Wallis test, $p < 0.0001$; Mann–Whitney *U* test, $^{**}p < 0.001$). 5-HT-labeled axon density is also significantly higher in SC-NSC-grafted spinal cords than in injured control animals ($^{**}p < 0.001$). ***N***, A longer growth distance of 5-HT axons is detected in BS-NSC- and SC-NSC-grafted animals compared with injured control animals (Kruskal–Wallis test, $p < 0.001$; Mann–Whitney *U* test, $^{*}p < 0.01$, $^{**}p < 0.001$), but the difference in maximum distance of 5-HT$^+$ axon growth does not reach significance (NS) between the two grafted groups ($p > 0.05$). ***O***, ***P***, Confocal 3D analysis shows 5-HT-labeled BS-NSC-derived projections in the IML expressing GFP (***O***) and the presynaptic marker synaptophysin (***P***; Syn). Scale bars: ***A–C***, ***E–G***, ***I–K***, 200 μm; ***D***, ***H***, ***L***, 25 μm; ***O***, 5 μm; ***P***, 2.5 μm.

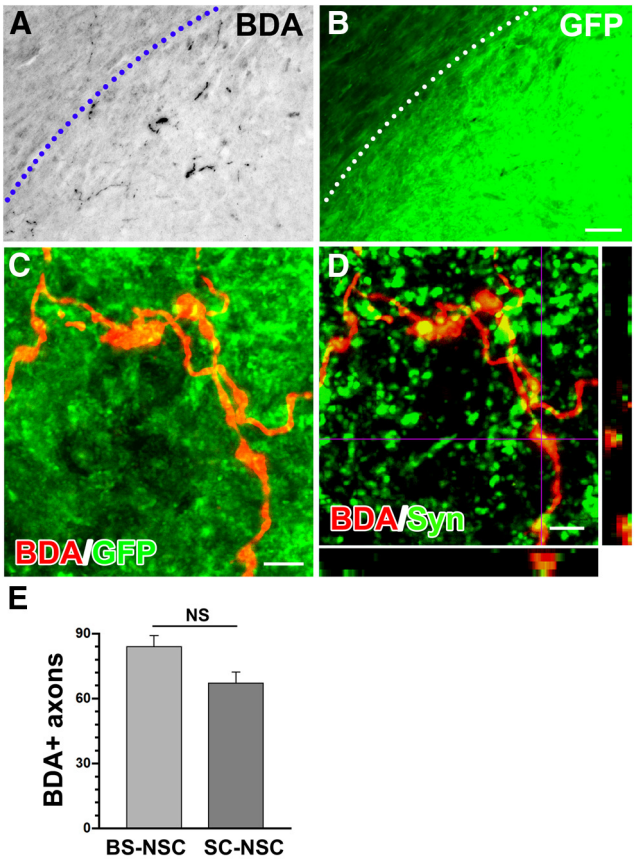

Figure 8. Host supraspinal projections connect with grafted BS-NSCs in the spinal cord. ***A***, ***B***, BDA-labeled rostroventrolateral medulla-derived vasomotor axons (black) regenerate into the graft identified by GFP immunolabeling (***B***, green). The host spinal cord/BS-NSC graft interface is indicated by a dotted line. ***C***, Confocal fluorescent microscopy demonstrates terminals of BDA-labeled descending projections (red) within BS-NSC implants, displaying bouton-like structures. ***D***, Confocal analysis reveals that the terminals of BDA-labeled fibers (red) in the graft colocalize (yellow) with the presynaptic marker synaptophysin (green), suggesting the formation of functional synapses. ***E***, Quantitative analysis shows that the number of BDA-labeled axons extending into BS-NSC grafts is not significantly (NS) different from those in SC-NSC grafts (unpaired *t* test, $p > 0.05$). Scale bars: ***A***, ***B***, 100 μm; ***C***, ***D***, 5 μm.

during embryo dissection. Despite their presence, a restoration of basal cardiovascular parameters was not observed in SC-NSC-grafted animals. Thus, a higher catecholaminergic and serotonergic input to SPNs as observed in BS-NSC-grafted animals might be necessary for the recovery of basal cardiovascular parameters.

During unpleasant visceral or sensory stimulation, autonomic dysreflexia develops when descending inhibitory control is lost as a result of a massive discharge of SPNs. A lack of vasodepressor responses via medullary catecholaminergic neurons is one of the mechanisms underlying the hyperreflexia (Reis et al., 1984). Furthermore, an inverse relationship between 5-HT immunolabeling in the IML and colorectal distension-induced cardiovascular responses in spinal cord contusion models indicates that a threshold of serotonergic axon density exists for the development of autonomic dysreflexia (Cormier et al., 2010). Colorectal distension-induced hypertension can also be suppressed by intrathecal administration of 5-HT_{2A} receptor agonists (Danzebrink and Gebhart, 1991; Cormier et al., 2010). In the present study, the magnitude of MAP increases during colorectal distension was significantly reduced after BS-NSCs and SC-NSCs were grafted to the spinal cord lesion site. Histological evidence in animals grafted with BS-NSCs suggests that dense TH^+ and 5-HT^+ inputs correlate to the mitigation of autonomic dysreflexia. However, in animals grafted with SC-NSCs, MAP increases were also significantly lower during colorectal distension-triggered autonomic dysreflexia despite much lower TH^+ and 5-HT^+ input. Possibly, the smaller number of SC-NSC-derived TH^+ and 5-HT^+ axons is sufficient to reduce MAP increases during colorectal distension but insufficient to normalize basal MAP. Alternatively, other graft-derived neurotransmitter phenotypes, such as GABA, glutamate, and substance P (Llewellyn-Smith, 2009), may also be involved in MAP restoration. Graft-derived inhibitory spinal interneurons could limit the reflexic sympathetic discharge. Spinal interneurons have been identified physiologically and anatomically to regulate the activity of SPNs. Although interneurons appear to play only a minor role in the intact spinal cord, they execute a more prominent role in the absence of bulbospinal pathways after SCI, generating ongoing sympathetic activity and mediating segmental or intersegmental sympathetic reflexes (Krassioukov et al., 2002; Schramm, 2006). Grafted SC-NSC-derived inhibitory input to spinal interneurons caudal to the lesion site could therefore be another mechanism for the reduced MAP increases after colorectal distension.

Several recent studies indicated that neuronal relays formed by implanted neural progenitors or fetal spinal cord stem cells can result in functional recovery, verified both electrophysiologically and behaviorally (Bonner et al., 2011; Lu et al., 2012). In the current study, cardiovascular functional recovery including resting parameters and colorectal distension-induced responses were abolished after spinal cord retransection above BS-NSC grafts. This suggests that signals above the graft are involved in rebuilding sympathetic regulation. This conclusion is further supported by two observations. First, grafted BS-NSCs extend axons caudally into the host spinal cord, which may provide direct or indirect input to SPNs; second, BDA-labeled rostroventrolateral medulla-derived vasomotor pathways penetrate the implants and display synaptophysin-labeled boutons within the graft. We selected the rostroventrolateral medulla as one representative nucleus to investigate host bulbospinal axon regeneration. In addition, other descending projections from medullary nuclei are also likely to innervate NSC grafts as demonstrated recently (Lu et al., 2012). Depending on the phenotype of relay neurons, supraspinal input to the graft might be relayed as excitatory or inhibitory signals to SPNs below the lesion site. The similar innervation of BS-NSC and SC-NSC grafts by BDA-labeled brainstem axons suggests that the phenotype of grafted cells strongly influences functional outcomes. Together, a neuronal relay by implanted BS-NSCs may provide a mechanism to reconstitute supraspinal sympathetic regulation and partial restoration of cardiovascular function after SCI.

We used a growth factor mixture to support initial graft survival. Growth factor proteins undergo rapid degradation but could have long-term effects on intraspinal plasticity. However, SC-NSC grafts were embedded in the same growth factor mixture as BS-NSC grafts, yet basal cardiovascular parameters were only normalized by BS-NSC grafts. Therefore, growth factors alone are unlikely to influence the investigated parameters. Furthermore, retransections abolished the functional recovery, suggesting that growth factor-mediated intraspinal plasticity below the lesion was not sufficient for the observed effects.

In summary, transplantation of embryonic brainstem neurons to control SPNs below a SCI site is potentially useful to reorganize vasomotor circuitry. Although our results demonstrate a profound influence on basal cardiovascular parameters and mitigated autonomic dysreflexia, animals still developed sig-

nificant responses to colorectal distension. To be of clinical relevance, a reduction in MAP increases as demonstrated in this study might be insufficient to avoid all cardiovascular consequences. Additional studies are needed to further decrease autonomic dysreflexia and to characterize the contribution of specific neurotransmitter phenotypes to the observed functional recovery using pharmacological approaches or transplantation of specified neuronal phenotypes.

References

Akhavan M, Hoang TX, Havton LA (2006) Improved detection of fluorogold-labeled neurons in long-term studies. J Neurosci Methods 152:156–162. CrossRef Medline

Bacon SJ, Smith AD (1988) Preganglionic sympathetic neurones innervating the rat adrenal medulla: immunocytochemical evidence of synaptic input from nerve terminals containing substance P, GABA or 5-hydroxytryptamine. J Auton Nerv Syst 24:97–122. CrossRef Medline

Basso DM, Beattie MS, Bresnahan JC (1995) A sensitive and reliable locomotor rating scale for open field testing in rats. J Neurotrauma 12:1–21. CrossRef Medline

Benarroch EE, Smithson IL, Low PA, Parisi JE (1998) Depletion of catecholaminergic neurons of the rostral ventrolateral medulla in multiple systems atrophy with autonomic failure. Ann Neurol 43:156–163. CrossRef Medline

Bonner JF, Connors TM, Silverman WF, Kowalski DP, Lemay MA, Fischer I (2011) Grafted neural progenitors integrate and restore synaptic connectivity across the injured spinal cord. J Neurosci 31:4675–4686. CrossRef Medline

Bruinstroop E, Cano G, Vanderhorst VG, Cavalcante JC, Wirth J, Sena-Esteves M, Saper CB (2012) Spinal projections of the A5, A6 (locus coeruleus), and A7 noradrenergic cell groups in rats. J Comp Neurol 520:1985–2001. CrossRef Medline

Cameron AA, Smith GM, Randall DC, Brown DR, Rabchevsky AG (2006) Genetic manipulation of intraspinal plasticity after spinal cord injury alters the severity of autonomic dysreflexia. J Neurosci 26:2923–2932. CrossRef Medline

Chalmers JP, Pilowsky PM, Minson JB, Kapoor V, Mills E, West MJ (1988) Central serotonergic mechanisms in hypertension. Am J Hypertens 1:79–83. CrossRef Medline

Coote JH (1990) Bulbospinal serotonergic pathways in the control of blood pressure. J Cardiovasc Pharmacol 15 [Suppl 7]:S35–S41.

Cormier CM, Mukhida K, Walker G, Marsh DR (2010) Development of autonomic dysreflexia after spinal cord injury is associated with a lack of serotonergic axons in the intermediolateral cell column. J Neurotrauma 27:1805–1818. CrossRef Medline

Dampney RA, Tagawa T, Horiuchi J, Potts PD, Fontes M, Polson JW (2000) What drives the tonic activity of presympathetic neurons in the rostral ventrolateral medulla? Clin Exp Pharmacol Physiol 27:1049–1053. CrossRef Medline

Danzebrink RM, Gebhart GF (1991) Evidence that spinal 5-HT1, 5-HT2 and 5-HT3 receptor subtypes modulate responses to noxious colorectal distension in the rat. Brain Res 538:64–75. CrossRef Medline

Furlan JC, Fehlings MG, Shannon P, Norenberg MD, Krassioukov AV (2003) Descending vasomotor pathways in humans: correlation between axonal preservation and cardiovascular dysfunction after spinal cord injury. J Neurotrauma 20:1351–1363. CrossRef Medline

Gaillard A, Prestoz L, Dumartin B, Cantereau A, Morel F, Roger M, Jaber M (2007) Reestablishment of damaged adult motor pathways by grafted embryonic cortical neurons. Nat Neurosci 10:1294–1299. CrossRef Medline

Grumbles RM, Sesodia S, Wood PM, Thomas CK (2009) Neurotrophic factors improve motoneuron survival and function of muscle reinnervated by embryonic neurons. J Neuropathol Exp Neurol 68:736–746. CrossRef Medline

Harris J, Lee H, Tu CT, Cribbs D, Cotman C, Jeon NL (2007) Preparing e18 cortical rat neurons for compartmentalization in a microfluidic device. J Vis Exp (8):305. CrossRef

Hasséssian H, Poulat P, Hamel E, Reader TA, Couture R (1993) Spinal cord serotonin receptors in cardiovascular regulation and potentiation of the pressor response to intrathecal substance P after serotonin depletion. Can J Physiol Pharmacol 71:453–464. CrossRef Medline

Hou S, Duale H, Cameron AA, Abshire SM, Lyttle TS, Rabchevsky AG (2008) Plasticity of lumbosacral propriospinal neurons is associated with the development of autonomic dysreflexia after thoracic spinal cord transection. J Comp Neurol 509:382–399. CrossRef Medline

Hou S, Lu P, Blesch A (2013) Characterization of supraspinal vasomotor pathways and autonomic dysreflexia after spinal cord injury in F344 rats. Auton Neurosci 176:54–63. CrossRef Medline

Inskip JA, Ramer LM, Ramer MS, Krassioukov AV (2009) Autonomic assessment of animals with spinal cord injury: tools, techniques and translation. Spinal Cord 47:2–35. CrossRef Medline

Jakeman LB, Reier PJ (1991) Axonal projections between fetal spinal cord transplants and the adult rat spinal cord: a neuroanatomical tracing study of local interactions. J Comp Neurol 307:311–334. CrossRef Medline

Jansen AS, Nguyen XV, Karpitskiy V, Mettenleiter TC, Loewy AD (1995) Central command neurons of the sympathetic nervous system: basis of the fight-or-flight response. Science 270:644–646. CrossRef Medline

Kalyani AJ, Rao MS (1998) Cell lineage in the developing neural tube. Biochem Cell Biol 76:1051–1068. CrossRef Medline

Karlsson AK (2006) Autonomic dysfunction in spinal cord injury: clinical presentation of symptoms and signs. Prog Brain Res 152:1–8. CrossRef Medline

Kisseberth WC, Brettingen NT, Lohse JK, Sandgren EP (1999) Ubiquitous expression of marker transgenes in mice and rats. Dev Biol 214:128–138. CrossRef Medline

Krassioukov AV, Johns DG, Schramm LP (2002) Sensitivity of sympathetically correlated spinal interneurons, renal sympathetic nerve activity, and arterial pressure to somatic and visceral stimuli after chronic spinal injury. J Neurotrauma 19:1521–1529. CrossRef Medline

Krassioukov AV, Furlan JC, Fehlings MG (2003) Autonomic dysreflexia in acute spinal cord injury: an under-recognized clinical entity. J Neurotrauma 20:707–716. CrossRef Medline

Krassioukov AV, Karlsson AK, Wecht JM, Wuermser LA, Mathias CJ, Marino RJ; Joint Committee of American Spinal Injury Association and International Spinal Cord Society (2007) Assessment of autonomic dysfunction following spinal cord injury: rationale for additions to International Standards for Neurological Assessment. J Rehabil Res Dev 44:103–112. CrossRef Medline

Krenz NR, Weaver LC (1998) Sprouting of primary afferent fibers after spinal cord transection in the rat. Neuroscience 85:443–458. CrossRef Medline

Laird AS, Carrive P, Waite PM (2006) Cardiovascular and temperature changes in spinal cord injured rats at rest and during autonomic dysreflexia. J Physiol 577:539–548. CrossRef Medline

Lindan R, Joiner E, Freehafer AA, Hazel C (1980) Incidence and clinical features of autonomic dysreflexia in patients with spinal cord injury. Paraplegia 18:285–292. CrossRef Medline

Llewellyn-Smith IJ (2009) Anatomy of synaptic circuits controlling the activity of sympathetic preganglionic neurons. J Chem Neuroanat 38:231–239. CrossRef Medline

Llewellyn-Smith IJ, Weaver LC, Keast JR (2006) Effects of spinal cord injury on synaptic inputs to sympathetic preganglionic neurons. Prog Brain Res 152:11–26. CrossRef Medline

Lu P, Wang Y, Graham L, McHale K, Gao M, Wu D, Brock J, Blesch A, Rosenzweig ES, Havton LA, Zheng B, Conner JM, Marsala M, Tuszynski MH (2012) Long-distance growth and connectivity of neural stem cells after severe spinal cord injury. Cell 150:1264–1273. CrossRef Medline

Mabon PJ, Weaver LC, Dekaban GA (2000) Inhibition of monocyte/macrophage migration to a spinal cord injury site by an antibody to the integrin alphaD: a potential new anti-inflammatory treatment. Exp Neurol 166:52–64. CrossRef Medline

Madden CJ, Morrison SF (2006) Serotonin potentiates sympathetic responses evoked by spinal NMDA. J Physiol 577:525–537. CrossRef Medline

Maiorov DN, Weaver LC, Krassioukov AV (1997) Relationship between sympathetic activity and arterial pressure in conscious spinal rats. Am J Physiol 272:H625–H631. Medline

Maiorov DN, Fehlings MG, Krassioukov AV (1998) Relationship between severity of spinal cord injury and abnormalities in neurogenic cardiovascular control in conscious rats. J Neurotrauma 15:365–374. CrossRef Medline

Marina N, Taheri M, Gilbey MP (2006) Generation of a physiological sym-

pathetic motor rhythm in the rat following spinal application of 5-HT. J Physiol 571:441–450. Medline

Marsh DR, Wong ST, Meakin SO, MacDonald JI, Hamilton EF, Weaver LC (2002) Neutralizing intraspinal nerve growth factor with a trkA-IgG fusion protein blocks the development of autonomic dysreflexia in a clip-compression model of spinal cord injury. J Neurotrauma 19:1531–1541. CrossRef Medline

Mathias CJ (2006) Orthostatic hypotension and paroxysmal hypertension in humans with high spinal cord injury. Prog Brain Res 152:231–243. CrossRef Medline

Minson JB, Arnolda LF, Llewellyn-Smith IJ (2002) Neurochemistry of nerve fibers apposing sympathetic preganglionic neurons activated by sustained hypotension. J Comp Neurol 449:307–318. CrossRef Medline

Mouchet P, Manier M, Dietl M, Feuerstein C, Berod A, Arluison M, Denoroy L, Thibault J (1986) Immunohistochemical study of catecholaminergic cell bodies in the rat spinal cord. Brain Res Bull 16:341–353. CrossRef Medline

Newton BW, Hamill RW (1988) The morphology and distribution of rat serotoninergic intraspinal neurons: an immunohistochemical study. Brain Res Bull 20:349–360. CrossRef Medline

Nout YS, Beattie MS, Bresnahan JC (2012) Severity of locomotor and cardiovascular derangements after experimental high-thoracic spinal cord injury is anesthesia dependent in rats. J Neurotrauma 29:990–999. CrossRef Medline

Rabchevsky AG, Patel SP, Lyttle TS, Eldahan KC, O'Dell CR, Zhang Y, Popovich PG, Kitzman PH, Donohue KD (2012) Effects of gabapentin on muscle spasticity and both induced as well as spontaneous autonomic dysreflexia after complete spinal cord injury. Front Physiol 3:329. Medline

Reier PJ, Bregman BS, Wujek JR (1986) Intraspinal transplantation of embryonic spinal cord tissue in neonatal and adult rats. J Comp Neurol 247:275–296. CrossRef Medline

Reis DJ, Granata AR, Joh TH, Ross CA, Ruggiero DA, Park DH (1984) Brain stem catecholamine mechanisms in tonic and reflex control of blood pressure. Hypertension 6:II7–II15. CrossRef Medline

Sawchenko PE, Bohn MC (1989) Glucocorticoid receptor-immunoreactivity in C1, C2, and C3 adrenergic neurons that project to the hypothalamus or to the spinal cord in the rat. J Comp Neurol 285:107–116. CrossRef Medline

Schramm LP (2006) Spinal sympathetic interneurons: their identification and roles after spinal cord injury. Prog Brain Res 152:27–37. CrossRef Medline

Schramm LP, Strack AM, Platt KB, Loewy AD (1993) Peripheral and central pathways regulating the kidney: a study using pseudorabies virus. Brain Res 616:251–262. CrossRef Medline

Stjernberg L, Blumberg H, Wallin BG (1986) Sympathetic activity in man after spinal cord injury. Outflow to muscle below the lesion. Brain 109:695–715. CrossRef Medline

Tang XQ, Heron P, Mashburn C, Smith GM (2007) Targeting sensory axon regeneration in adult spinal cord. J Neurosci 27:6068–6078. CrossRef Medline

Teasell RW, Arnold JM, Krassioukov A, Delaney GA (2000) Cardiovascular consequences of loss of supraspinal control of the sympathetic nervous system after spinal cord injury. Arch Phys Med Rehabil 81:506–516. CrossRef Medline

Weaver LC, Marsh DR, Gris D, Brown A, Dekaban GA (2006) Autonomic dysreflexia after spinal cord injury: central mechanisms and strategies for prevention. Prog Brain Res 152:245–263. CrossRef Medline

Willerth SM, Faxel TE, Gottlieb DI, Sakiyama-Elbert SE (2007) The effects of soluble growth factors on embryonic stem cell differentiation inside of fibrin scaffolds. Stem Cells 25:2235–2244. CrossRef Medline